SSC-236

The Superconducting Super Collider

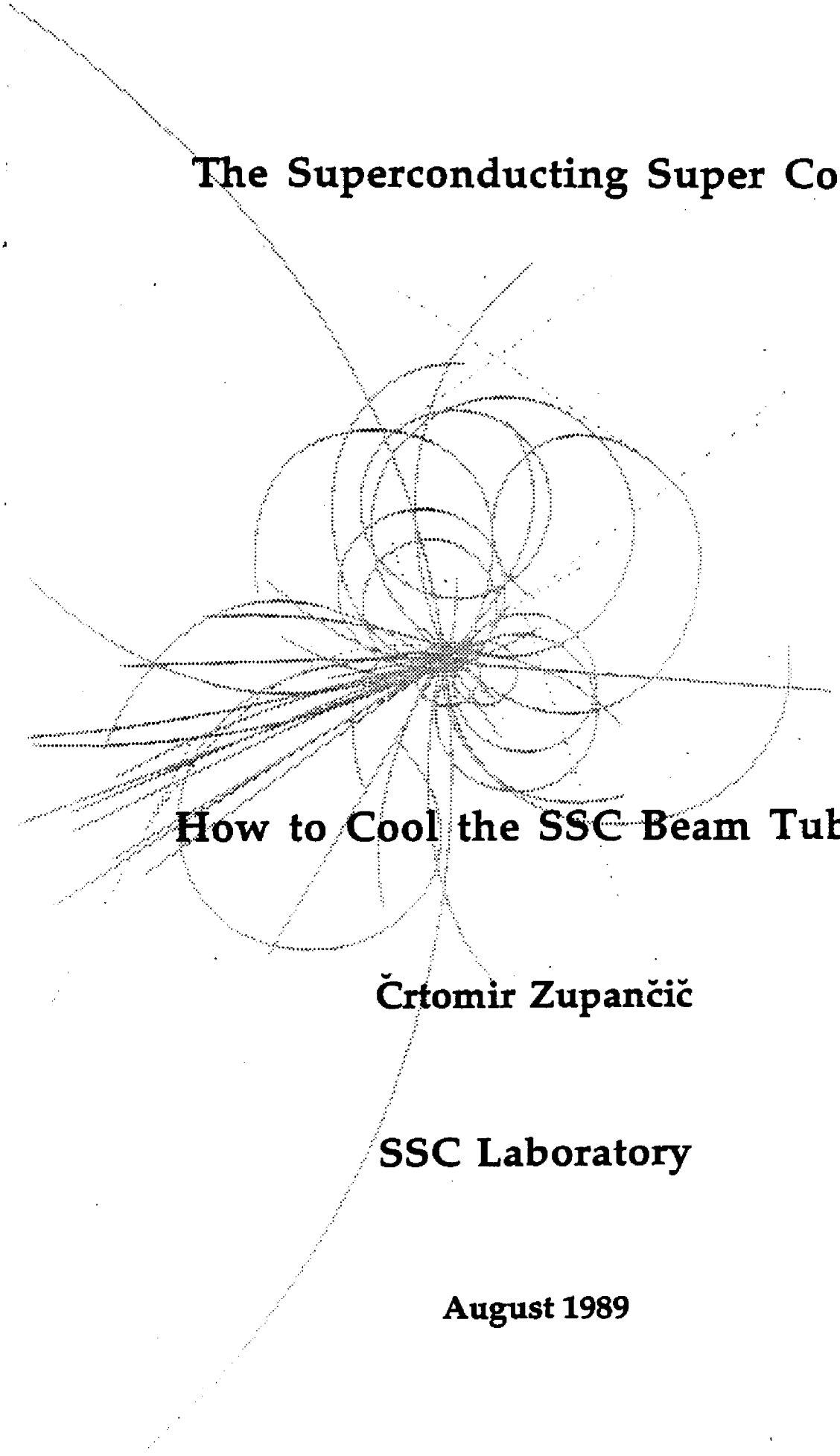

How to Cool the SSC Beam Tube?

Črtomir Zupančič

SSC Laboratory

August 1989

SSC-236

The Superconducting Super Collider

How to Cool the SSC Beam Tube?

Črtomir Zupančič

SSC Laboratory

August 1989

SSC-236

HOW TO COOL THE SSC BEAM TUBE ?

Črtomir Zupančič

Sektion Physik
LM Universität München
D 8046 Garching, FRG

and

SSC Central Design Group*
Lawrence Berkeley Laboratory
Berkeley CA 94720, USA

August 1989

The cooling of the beam tube according to the present SSC design is reexamined, and previous conclusions about its inadequacy are confirmed. Two methods for improved cooling are discussed: transverse helium flow and a metallic heat shunt. Under the nominal heat load of 0.142 W/m, both methods should be capable of limiting the temperature rise of the superconductor with respect to the helium in the yoke channels to about 0.02-0.03 K. The implementation of both methods in parallel is possible.

* Operated by Universities Research Association, Inc., for the U.S. Department of Energy.

1. Introduction

The temperature of the superconductor in a dipole magnet is a crucial parameter of a superconducting accelerator. It is determined by the heat deposited during the operation of the accelerator in different parts of the cold mass, by the properties of these parts, and by the cooling method. In the present SSC design, as documented in the Conceptual Design Report (CDR) [1], the heat leak from outside to the cold mass at 4 K* is expected to amount to about 0.02 W/m. It is readily absorbed by the liquid helium flowing in the yoke channels and thus does not directly affect the temperature of the superconductor. On the other hand, the beam heats the superconductor directly through showers caused by beam losses and by heating the beam tube, which is cooled at least partly (in the present design mainly) by conduction through the coil-collar-yoke assembly. We shall refer to beam-related heat as "internal" heat.

The main source of internal heat at 20 TeV is synchrotron radiation. With 1.27×10^{14} protons/ring, 0.142 W/m is deposited along a narrow strip on the outer rim of the inner surface of the beam tube. At 20 TeV, parasitic heating of the beam tube contributes less than 1%, but beam-gas interactions have been estimated to add another 5% of the synchrotron radiation power. However, this latter value depends on the residual gas pressure, which may vary around the ring; on particle cross sections at energies up to 20 TeV; and on a Monte Carlo calculation of shower development. Clearly, it should be considered more an order-of-magnitude estimate than a solid number. During ramping, additional heat is generated in the cold mass, mainly due to hysteresis in the iron and in the superconductor; each contributes about 0.02 W/m.

One reason to prevent the temperature of the superconductor in the SSC dipole magnets from rising above the design value of 4.35 K is obvious. At

* For simplicity, we write 1 K instead of 1°K, 1 mK instead of 0.001°K, and 1 m-K instead of 1 meter × 1°K.

4.35 K, the logarithmic derivative with respect to temperature of the "short-sample" value B_{ss} of the central dipole field is [2]

$$\frac{1}{B_{ss}} \frac{dB_{ss}}{dT} = -0.17 \text{ K}^{-1} . \tag{1.1}$$

Any increase in temperature causes a decrease in the achievable dipole magnetic field, i.e., a proportional decrease in proton energy.

In the present design and at 20 TeV, the 4 K cooling system works with a temperature difference of about 170 mK between the coldest and warmest supercritical helium in the yoke channels [3]. This value has been calculated by taking into account the heat loads of all elements – not only the dipole magnets – in a cryogenic sector, and the cooling effect of the recoolers on the 100 g/s supercritical helium flow in the yoke channels.

The annular passage around the beam tube with the nominal width of 1.4 mm is traversed nominally by 1 g/s of supercritical helium; the actual helium flow is probably smaller, since the passage is obstructed by spacers and additional insulators. This flow is by far too small to limit the temperature rise of the superconducting coil along the entire length of a dipole magnet below the value imposed by heat conduction through the cold mass from the coil to the yoke channels. The latter value has been estimated [4] at roughly (another) 170 mK. Carcagno [5] has convincingly argued that the vertical gaps in the collar do not cause any appreciable mixing of the helium in the annulus and the helium in the yoke channels. The helium in the annulus may to some extent serve to spread the internal heat around the azimuth. However, this effect has not yet been quantitatively estimated; the mixed convection in the turbulent helium flow in an obstructed annulus defies analysis. Ref. [4] simply assumes that the the spreading is perfect so that the temperature in the annulus is independent of azimuth.

The above values of temperature differences indicate that, at 20 TeV, the warmest part of the superconductor might have a temperature near 4.5 K rather than 4.35 K as aimed at in the design [1]. The simplest (though perhaps not the

most economical) way to reach the design value would be to increase the refrigerating capacity. However, this solution is not satisfactory, because the operation of a superconducting accelerator depends not only on the absolute temperature of the superconductor but also on its variations in space and time. The reason for that is the temperature dependence of the superconductor magnetization, i.e., of persistent currents [6]. They affect the sextupole component of the magnetic field and, through it, the chromaticity of the accelerator, and they are particularly worrisome at low fields, i.e., at injection. There, unforeseen beam losses, potentially resulting in substantial heat deposition in the superconductor, are a constant threat. Indeed, this is a major problem for the operation of a superconducting accelerator [7]. Beam losses in combination with the temperature dependence of chromaticity constitute a positive feedback mechanism driving the accelerator into instability. This mechanism could push the upper limit of tolerable beam losses (at least of non-localized ones) well below the value expected from direct quenching considerations; however, it has not yet been investigated in detail.

The time dependence of superconductor temperature after a sudden heat deposition is a more complicated topic than the cooling of the beam tube, and merits a separate discussion. However, minimizing the heat that flows from the beam tube into the superconductor is desirable in itself. To the extent that this is achieved by lowering the temperature at the outer surface of the coils, and not by increasing their thermal insulation, it also helps to cool the irradiated superconductor.

In the present Note, I discuss two improvements of the cooling method: transverse helium flow and metallic heat shunts. Their respective merits are complementary, and one may envisage implementing both of them in parallel. To facilitate understanding, I first analyze the cooling of the cold mass in the present design. This analysis is presented in Section 3, preceded by a short Section 2, which summarizes the thermal conductivities used in the calculations. Section 4 describes one of the several possible ways of implementing transverse helium

flow, while Section 5 presents a simple heat shunt. The discussion in these two Sections is on the level of conceptual design criteria and order-of-magnitude estimates, i.e., very far from a concrete engineering design. Section 6 offers some suggestions for experimental tests, while section 7 contains the conclusions and a few additional remarks. Mathematical details are relegated to Appendices. Appendices A, B, and C deal with heat conduction; Appendix D presents the solution of a relevant eddy-current problem.

2. Material properties

All quantitative estimates in this Note depend on the thermal conductivities k assumed for different materials. Table 1 states the values I work with; they are essentially identical to those used in ref. [5] , except perhaps for copper. Some values of k have been slightly adjusted (within their uncertainties), in order to make them simple fractions of k(Cu). The uncertainties about the conductivities of copper and Kapton are well known. Actually, high-purity aluminum may be a better material than copper for the conductor of the heat shunt but, unfortunately, it is more sensitive than copper to mechanical stress [8]. However, the assumed value of k(Cu) should represent a lower bound of attainable conductivities of both copper and aluminum.

Table 1.

Assumed thermal conductivities k at 4.3 K in units W/(m-K) and their ratios to k(Cu)

Material	k	k/k(Cu)
Copper (B=6T)	260	1
Iron	2.6	1×10^{-2}
Stainless steel	0.26	1×10^{-3}
G10 (or glue)	0.078	3×10^{-4}
Teflon	0.052	2×10^{-4}
Liquid He	0.026	1×10^{-4}
Kapton	0.0052	2×10^{-5}

3. Heat flux and temperature distribution in the present design

The cross section of the cold mass in the present design is shown in Fig. 1. In the following, we shall use the term "temperature rise of the coil" for the temperature difference between the warmest part of the superconductor and the helium in the yoke channels at the same longitudinal position in the magnet. We shall assume a nominal deposition by synchrotron radiation of 0.142 W/m of heat along the beam tube; *all values of temperature differences to be quoted refer to this nominal value of the heat source,* unless stated otherwise.

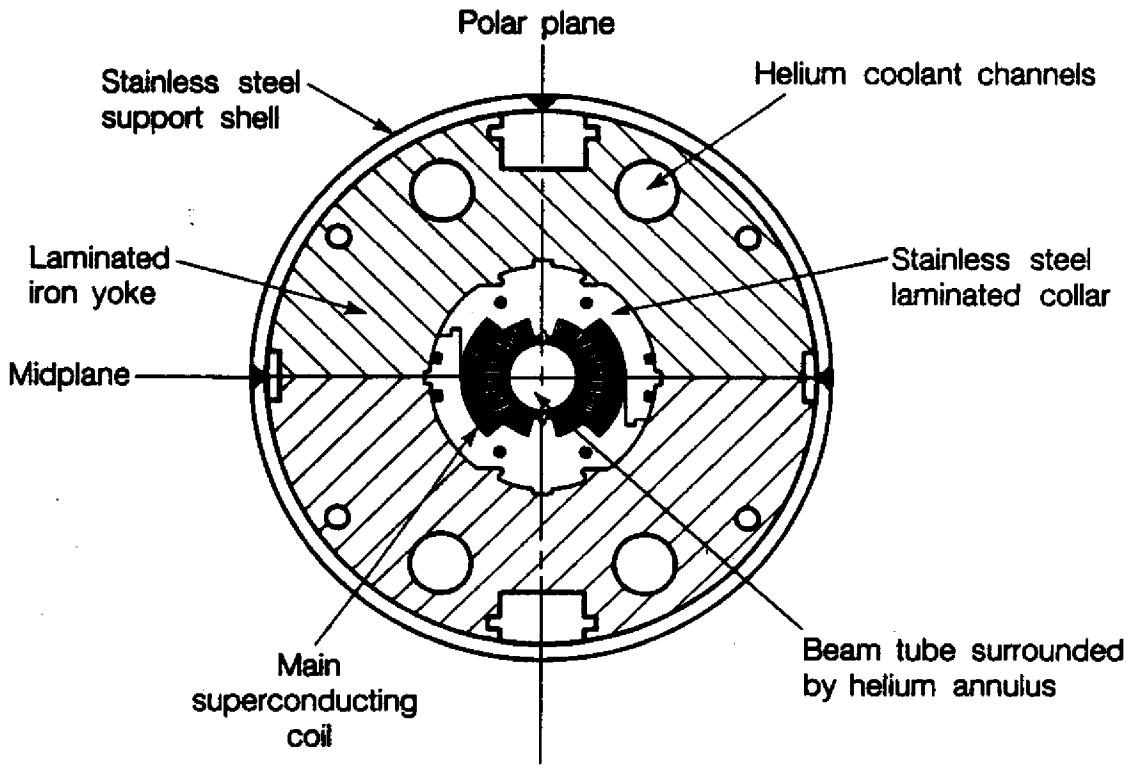

FIG. 1. Cross section of the central part ("cold mass") of the SSC dipole magnet. The inner radia of the different parts are approximately as follows: beam tube 1.6 cm, inner coil 2 cm, outer coil 3 cm, iron yoke 5.5 cm, support shell 13.3 cm.

The heat flux through a copper-lined beam tube and the resulting temperature distribution on the inner surface of the beam tube heated by synchrotron

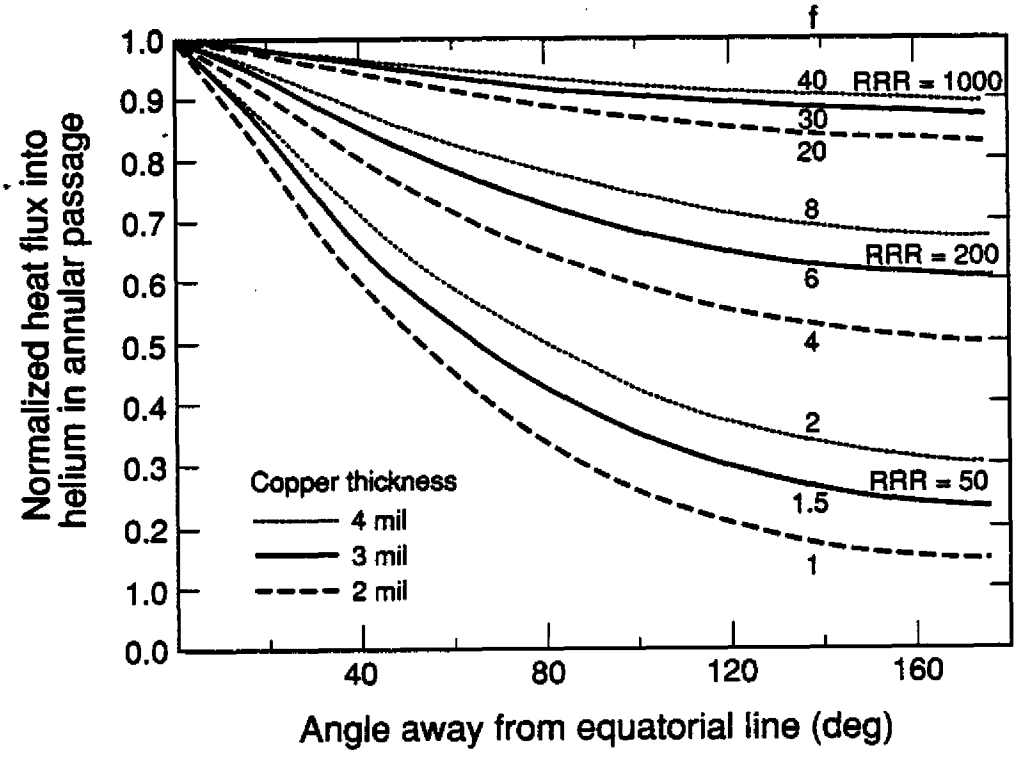

FIG. 2. Azimuthal distribution of the normalized radial heat flux through the beam tube irradiated by synchrotron radiation, as calculated by Carcagno [5]. Since the outer surface of the beam tube is assumed to have a constant temperature, the curves also represent the azimuthal distribution of the normalized temperature in the copper lining on the inner surface. The parameters are the RRR of the copper lining and its thickness t. The product of these two parameters relative to $RRR = 50$ and $t = 2\,\text{mil}$ is called f, i.e., $f = t \times (RRR)/(2\,\text{mil} \times 50)$.

radiation have been calculated by Jackson [9]. He assumes a constant temperature in the helium annulus, which makes the problem independent of the properties of the coil-collar-yoke assembly; however, as mentioned in the Introduction, the validity of this boundary condition in a real dipole magnet is very questionable. The two-dimensional treatment of ref. [9] has been extended from Cartesian to cylindrical coordinates by Carcagno [5]. Fig. 2 presents his results on the heat flux as a function of azimuth for different values of residual resistivity ratio RRR and thickness t of the copper lining; the additional quoted values of the parameter

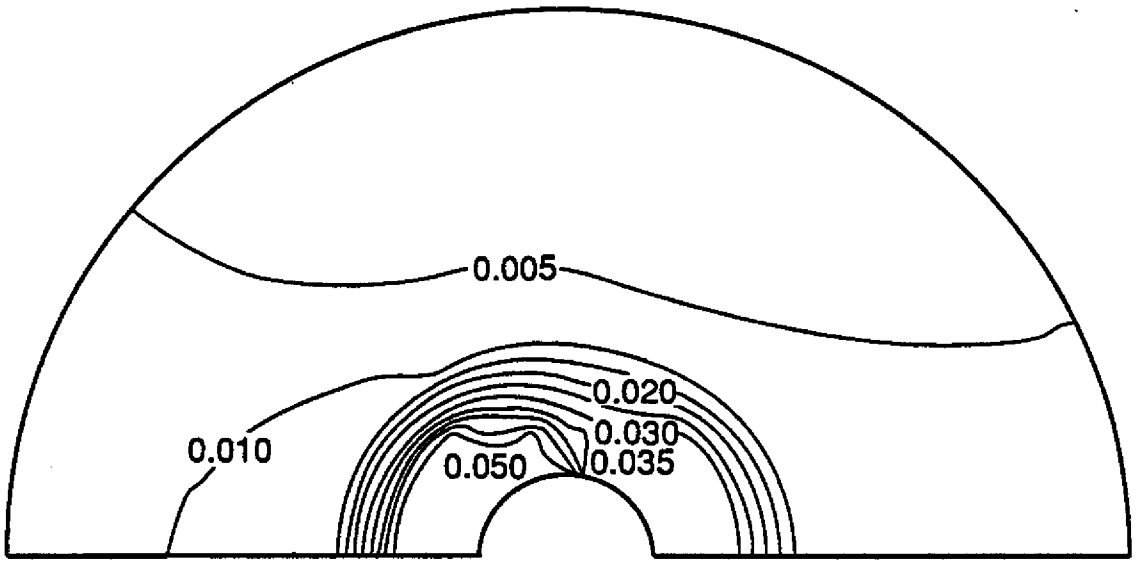

FIG. 3. Isotherms in an idealized cold mass at radii $2\,\mathrm{cm} \leq r \leq 5.5\,\mathrm{cm}$, with no insulators and unrealistic boundary conditions at the surface $r = 2\,\mathrm{cm}$, as calculated by Carcagno [5]. The mirror image of his Fig. 2 is shown here, in order to be directly comparable to our Fig. 2 where the temperature maximum is also on the left side of the figure.

f are those of the product $(RRR)\,t$ relative to $RRR = 50$ and $t = 2$ mil. Fig. 2 could also be obtained from the simpler one-dimensional treatment presented in appendices A-C (see eq (C11)).

Carcagno [5] has also performed an interesting finite-element analysis of the temperature field in the coil-collar-yoke assembly, the results of which are reproduced in Fig. 3. He has omitted all insulating materials and all contact thermal resistances. Also, he has imposed an inconsistent boundary condition in the annulus in that he requires the heat flux at radius $r = 2\,\mathrm{cm}$, i.e., at the inner coil surface, to be given by the curve corresponding to $f = 1.5$ in Fig. 2. Since the latter has been calculated by assuming an azimuth-independent temperature in the annulus, a heat flux distribution at $r = 2\,\mathrm{cm}$ that is consistent with this assumption does not depend at all on the flux through the beam tube; in particular, it cannot lead to a left-right asymmetry of the temperature field such as

seen in Fig. 3. On the other hand, if the temperature distribution in the annulus were left free, the helium in the yoke channels would act as the only heat sink of constant temperature (at a given longitudinal position). Then, the temperature and heat current fields in the cold mass would depend on the geometry and thermal conductivity of all of its constituents. For instance, if the annulus is assumed to be filled by a stationary solid, the thermal resistance of the annulus-coil-collar-yoke assembly has to be added to that of the beam tube when calculating the temperature distribution in the copper lining of the inner tube surface. The heat then "takes advantage" of the increased thermal resistance to radial flow in order to distribute itself more uniformly in the copper lining; this leads to a more isotropic distribution of heat flux through the beam tube than presented in Fig. 2.

However, Fig. 2 is still very useful if one wants to know the azimuthal distribution of the heat flux from the beam tube for different values of the total thermal resistance between the inner surface of the beam tube and the helium channels in the yoke. We define the thermal resistance/(unit length) as the temperature difference between two isothermal closed curves in the magnet cross section, traversed by the nominal synchrotron-radiation heat flux/(unit length) of 0.142 W/m. With our definition, thermal resistances are measured in temperature units. The only problem with that is the risk of confusion between thermal resistance and actual temperature differential. In the definition of resistance we have to impose a constant temperature on each of the two closed curves; this boundary condition determines the temperature and heat current field in the plane between them. In the actual problem that we are trying to solve, these fields may be different. However, when the difference is either small or well known, one can still reliably estimate the actual temperature differential if one knows the thermal resistance.

To minimize the risk of confusion, we shall adopt the symbol 'mK' (to be pronounced, for instance, "millikelvin equivalent" or "quasiemkay") for the unit of thermal resistance. Fig. 1 has been calculated assuming a tube resistance of

31 'mK'. It follows from appendices A-C that increasing this resistance by a factor f, while keeping the copper lining fixed, has the same effect on the azimuthal flux distribution as increasing the product of the copper RRR and the thickness t of the lining by the factor f, while keeping the value of the total thermal resistance constant. The thermal resistance of the beam tube in the present design is 54 'mK' and, if we assume the resistance of the remaining assembly to be, e.g., 132 'mK', $f = (132 + 54)/31 = 6$. In Fig. 1, the curve for $RRR = 200$ with a thickness of 3 mil corresponds to $f = 6$. It may be roughly characterized by the ratio $R =$ (maximum radial heat current)/(average current) $= 1.33$.

When looking at Fig. 3, it is easy to imagine a temperature field with smaller left-right asymmetry. However, it is not as straightforward to correct for the lack of insulators. In Fig. 3, the thermal conductivity of the coils is effectively infinite, and the temperature gradients are different from zero only in the stainless steel and in the iron. In reality, the average thermal conductivity of the coils, including the insulating tapes, is quite low. Unfortunately, it is different in the radial and the azimuthal direction, which complicates its insertion in standard finite-element programs. In order to obtain the average thermal conductivity of the coils in the radial direction, the local radial resistivity at given azimuth has been computed by properly averaging (in cylindrical coordinates) the insulator resistivities over both inner and (where applicable) outer coil and neglecting the resistivity of the copper-superconductor wire. These local resistivities have been inverted and averaged over the relevant range in azimuth, separately for the azimuthal region with only the inner coil and the region containing both coils. Within 10%, both resulting values of average radial coil conductivity are the same and equal to

$$k(\text{coils, radial}) = 0.5\ k(\text{stainless steel}). \tag{3.1}$$

The average conductivity in the azimuthal direction has been determined in an analogous but slightly simplified way, by adding the insulator resistances at constant radius of 2.5 cm for the inner coil and 3.5 cm for the outer coil. The

average conductivity is obtained by comparing these added resistances with the resistances of imaginary coils made of stainless steel. The average azimuthal conductivity of the inner coil is about 1.4 times higher than that of the outer coil, but for qualitative arguments it suffices to quote a round value nearer to the lower of the two conductivities

$$k(\text{coils, azimuthal}) = 0.2\ k(\text{stainless steel}). \tag{3.2}$$

Thus, contrary to Fig. 3, the average coil conductivities are in reality considerably lower than the conductivity of stainless steel. As a consequence, the temperature field is different from the one shown in Fig. 3. In particular, there are large temperature gradients inside the coils, and there is much less heat flow from the right half of the assembly to the left one. This latter fact is a consequence of a simple rule governing heat flow, analogous to Snell's law in optics: from the continuity of the temperature and of the normal component of the heat current at the boundary between two media, it follows that

$$\frac{k_1}{\tan\alpha_1} = \frac{k_2}{\tan\alpha_2} \tag{3.3}$$

(see Fig. 4). We see that in traversing the boundary from a medium with high thermal conductivity into another medium with vastly lower conductivity, the heat current has the tendency to become nearly normal to the boundary surface. This is the reason why in Fig. 3 the heat current, as it reaches the right boundary of the left coil (assumed to have very high conductivity), is directed across the stainless steel "nose" towards the right coil and – in the absence of total reflection (contrary to optics) – tends to enter the right coil. The opposite situation occurs with the real coil. The current passing from the left coil into the stainless steel "nose" will be deflected into the radial direction and will flow through the stainless steel to the yoke. As a consequence, there will be much less mixing of the heat fluxes from the two halves of the assembly. Since, in addition, the coil

conductivity is twice as low in the azimuthal than in the radial direction, the heat flux mixing within each half will be reduced, as well. These effects tend to partly compensate for the consequences of the inconsistent boundary condition at $r = 2\,\mathrm{cm}$ in Fig. 3.

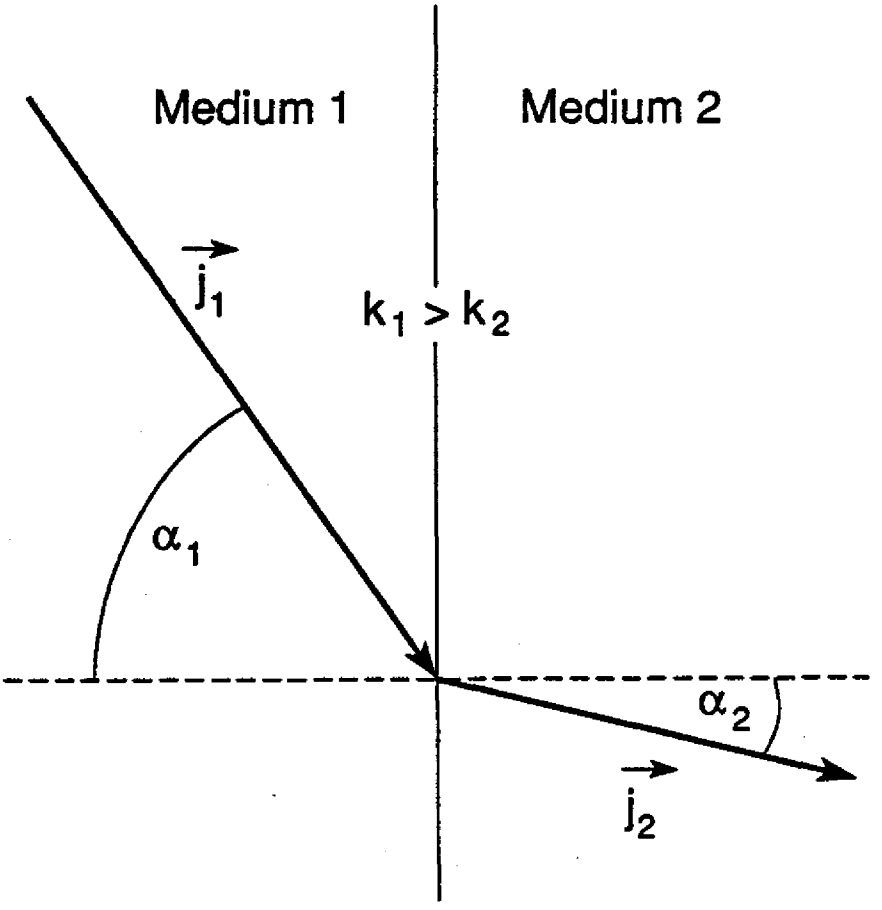

FIG. 4. The "refraction" of lines of heat current $\vec{j}$ at the boundary between two materials with different thermal conductivity k.

The GD report [4] called attention to a substantially larger coil temperature rise than estimated in the Conceptual Design Report [1] . It was immediately realized [10] that the larger rise was due mainly to new, extremely low values of Kapton thermal conductivity; (actually, the GD report assumes a 10% lower

Kapton conductivity than quoted above in section 2). The GD report imposes the boundary condition of azimuth-independent temperature in the annulus; it can be criticized in other respects as well. On the other hand, the calculational tool provided with the report is very flexible and is being presently used by Carcagno to recalculate the temperature field in the cold mass [11]. However, it is difficult to guarantee the correctness of a large amount of computer code and of the large bank of data it requires as input. Therefore, a rough check by a back-of-the-envelope estimate of the temperature rise is still desirable.

This estimate is documented in Table 2. The convective resistance of the four yoke channels in parallel has been calculated from the Dittus-Boelter equation as evaluated in ref. [8]. The convective resistance of the narrow annular gap, assumed to be 12 mil wide, between the yoke and the collar has been determined from eq (8-26) and Table 8-1 in the book of Kays [12] and found to be equal to the thermal resistance of a stationary helium layer. The temperature differentials corresponding to these two convective resistances have been estimated by making some rough guesses about the local nonuniformity of the heat flux; the azimuthal flux distribution at the collar-yoke interface is most probably more uniform than in Fig. 3, but peaked at the polar plane rather than at the midplane. No account has been taken of the ill-defined and (let us hope) small convective resistances in the coils themselves and between coils and collar; temperature differentials across boundaries between different materials of the cold mass, as expected from acoustic mismatch [13], [14], are believed to be small at 4 K and have been neglected. The convective resistance of the annular passage between the beam tube and the coil-collar assembly has been estimated (neglecting obstructions) from eq (8-26) and Table 9-5 of ref. [12] by taking the Reynolds number $Re = 10000$ and the Prandtl number $Pr = 0.56$.

The temperature differential across the iron yoke has been read off Fig. 3. It is more difficult to obtain a good estimate of the effective thermal resistance of the complicated coil-collar assembly. However, one can find its lower and upper bound. The lower bound is obtained by assuming that the concentric

Table 2.

Thermal resistances in 'mK' and the temperature differentials in mK of the present design

Body or interface	Thermal resistance	Temperature differential
4 yoke channels in parallel (convective)	0.9	3
Yoke		11
Gap between yoke and collar	0.4/mil	6
Coil-collar assembly (without one cable insulation layer)		135
Total temperature rise of the coil		155 ± 15
One layer of cable insulation		11
Annulus (convective)	13	19
Beam tube	54	85
Temperature differential between coil and inner surface of the beam tube		115 ± 15
Total temperature differential between helium in yoke channels and inner surface of the beam tube		270 ± 20

cylindrical surfaces at radia $r = 2$ cm, $r = 3$ cm, $r = 4$ cm, and $r = 5.5$ cm are isothermal (with temperatures different from each other, of course). This is essentially equivalent to assuming zero "circumferential" (azimuthal) resistances in the GD model. The resulting lower bound, obtained by taking all insulators into account as well as possible, is 112 'mK'. This value can be used to find the upper bound for the azimuthal flux nonuniformity, obtaining $f = 5.8$, which corresponds to the ratio $R = 1.36$. Multiplying this ratio by the resistance of inner coil, outer coil, and a 1.5-cm-thick stainless steel cylinder in series (with insulator thicknesses taken at an azimuth of about 40° with respect to the midplane) yields the upper bound of 190 'mK'. This procedure is roughly equivalent to setting all circumferential resistances in the GD model to infinity and correcting for the

upper bound of flux nonuniformity from the beam tube.

From here on, it is anybody's guess. Our lower bound certainly overestimates the azimuthal mixing of heat flux in the annulus-coil-collar assembly, while the upper bound just as certainly underestimates it. Perhaps, taking the geometric mean of the two bounds, i.e., 146 mK, is as good a guess as any of the temperature diferential across the coil-collar assembly. About one sixth of the difference between the two bounds, i.e., 13 mK, may be a fair estimate of the standard deviation of this value. However, the temperature differential across one layer of cable insulation (about 11 mK) has to be subtracted to obtain the final value of the total temperature rise of the warmest part of the coil.

The additional temperature differential between coil and inner surface of the beam tube is of interest for estimating the temperature of correction coils and the degassing of the tube under synchrotron radiation. If an azimuth-independent temperature in the annulus is assumed, the maximum temperature differential across the beam tube is obtained by multiplying 54 'mK' by the R-factor corresponding to $f = 54/31$, i.e., $R = 2$. In the opposite extreme, a maximum f-factor may be estimated to be $f = (190 + 11 + 54)/31 \approx 8$ corresponding to $R = 1.24$. Taking again the geometric mean of the two R-values as the best guess, one obtains the values quoted in Table 3; the value estimated for the temperature differential across the annulus is certainly even more uncertain than the others. The quoted standard deviations are informed guesses, at best.

The two GD assumptions that are different from ours, i.e., 10% lower Kapton thermal conductivity and no azimuthal dependence of the temperature in the annulus, have opposite effects on the temperature rise of the coil. The value quoted in Table 3 is lower than the GD estimate, but the difference is well within the combined errors of both evaluations. The comparison with the new calculation of Carcagno[11] is equally favorable.

In view of a potential replacement of the present brand of Kapton by an insulator with higher thermal conductivity, it is of interest to repeat the above

estimates with increased values of k(Kapton) but with all other parameters unchanged. Choosing two values, one a factor of 3.16 and the other a factor of 10 higher than the present k(Kapton), one obtains the values (75 ± 4.5) mK and (55 ± 3.5) mK, respectively, instead of the value 135 mK of Table 3; the quoted standard deviation represents 1/6 of the difference between the upper and the lower bound in each case. This translates into a temperature rise of the coil of 95 mK and 75 mK, respectively. We see that even substantially increased values of Kapton conductivity (which make the average radial conductivity of the coil higher than that of stainless steel) are not likely to yield the value of 55 mK expected in the CDR [1] for the coil temperature rise. The temperature difference between the warmest spot of the coil and the warmest spot of the beam tube is also reduced to 85 mK and 75 mK, respectively, which leads to a total temperature differential between helium in the yoke channels and inner surface of the beam tube of 180 mK and 150 mK, respectively.

4. Transverse helium flow

Transverse helium flow is potentially a much more efficient means of cooling superconducting magnets than longitudinal flow [8]. For SSC dipole magnets, transverse helium flow has been advocated by Shutt [15]. Recently, Shutt [16] and Rehak [17] have proposed a detailed design of the cooling system and calculated its expected response. The proposal requires minimal changes of the present design by making ingeneous use of the collar pickup notches* to connect the vertical gaps in the yoke with the analogous gaps in the collar (the two sets of gaps are not aligned, in general, according to the present design). The helium flow is made partially transversal by installing flow-obstructing orifices at the entrance of the lower pair of yoke channels and at the exit of the upper pair. In this way, the flow along the magnet is gradually redirected from the upper pair to the lower one. The expected temperature rise depends on the choice of several

* Fig. 1 is not sufficiently detailed to show that the four notches, which are nearer the polar plane than the midplane, are actually not obstructed by iron.

parameters (for example, the diameter of the orifices), but it should be of the order of 20 mK.

The transverse cooling design proposed by Shutt and Rehak may be criticized on the grounds that local mishaps, like annulus clogging, could have global repercussions along an entire string of magnets. Also, the helium pressure may have to be increased more than the minimum required to guarantee sufficiently strong helium flow. An alternative scheme that may avoid these shortcomings has been suggested [18], but only as a concept, not as an engineering design. Here, it is presented again, since it is sufficiently different from the Shutt-Rehak proposal to merit some attention.

The principle is schematically shown in Fig. 5. We assume that the present 1/16-inch gaps at 6-inch intervals are extended in some way through the yoke to the helium channels. The detailed design of this extension depends on, among other things, the final mechanical design of the collar-yoke assembly. Simple baffles, shown schematically by dashed lines in Fig. 5 and in more detail in Fig. 6, ensure that the entire helium in the annulus around the beam tube returns to a pair of yoke channels after 6 inches and is replaced by helium from the other pair of channels. In this scheme, the turbulent flow in the channels should guarantee complete helium mixing and therefore optimal cooling of the beam tube.

In spite of the increased flow resistance, the present helium flow in the annulus of 1 $\mathrm{g\,s^{-1}}$ (i.e. a velocity of about 5 $\mathrm{cm\,s^{-1}}$) may be attainable with a minimal increase of the external pressure differential. At present, the helium velocity in the channels is about 30 $\mathrm{cm\,s^{-1}}$; the corresponding hydrodynamic pressure $p = \rho v^2/2$ (ρ is density, v is velocity) is about 10 $\mathrm{N\,m^{-2}}$ or 0.0001 atm. This value is large compared with the drop in external pressure over a distance of 6 inches, about 1.3 $\mathrm{N\,m^{-2}}$. Ensuring that the helium velocity at the entrance to the 1/16-inch-wide vertical gap is substantially less than 30 $\mathrm{cm\,s^{-1}}$ and – if necessary – that it is substantially larger than this value at the exit from the next vertical gap should not prove too difficult. Suitable constrictions in the

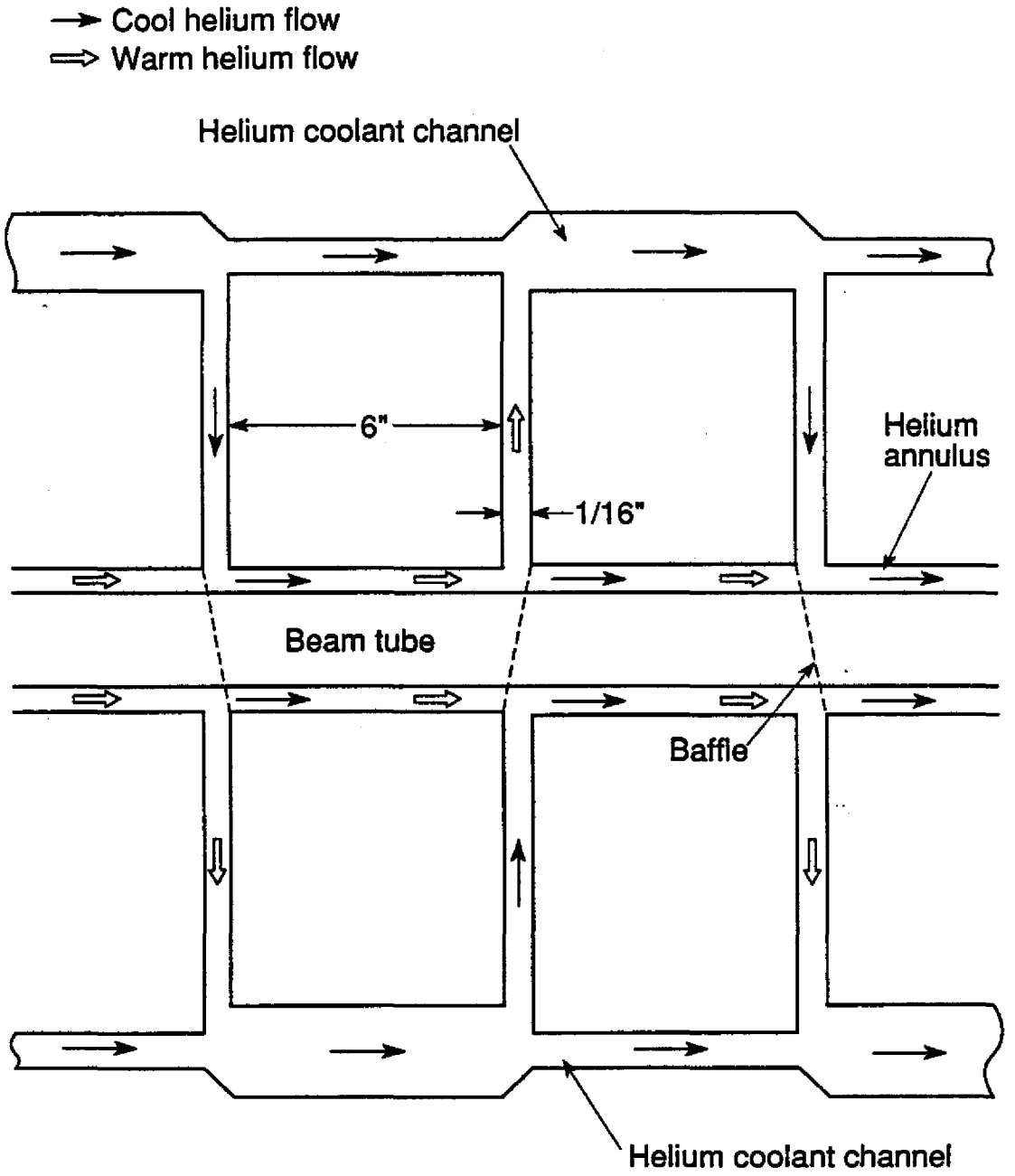

FIG. 5. Schematic diagram of the proposed transverse cooling method.

yoke channels could achieve velocity differences resulting in pressure differences of several $\mathrm{N\,m^{-2}}$ without drastically increasing the flow resistance of the channels.

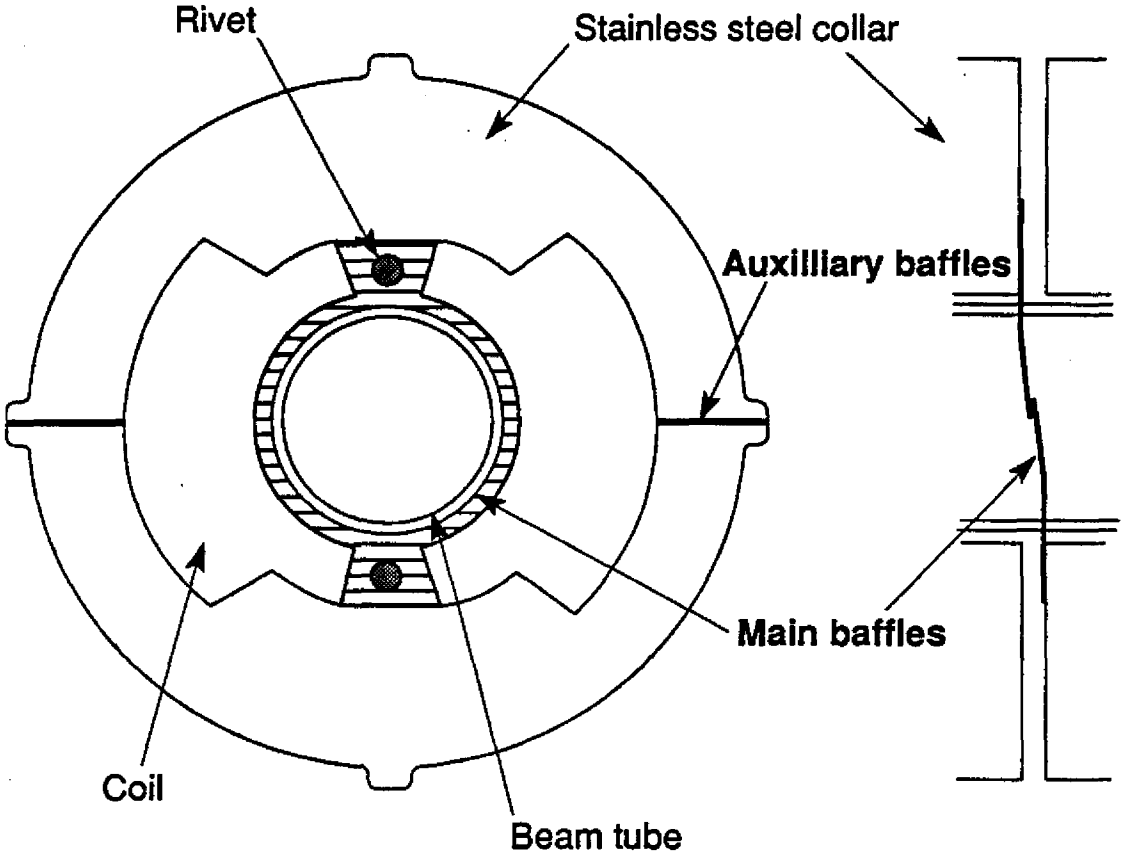

FIG. 6. A possible design of baffles ensuring the helium flow of Fig. 5. The view in the beam direction shows the horizontally hatched main baffles in the annulus and the auxilliary baffles outside the coils. The latter may have to be extended into a yoke gap. The collar pickup notches would have to be plugged as well. The main baffles are better discernible in the polar cross section, i.e., in the view perpendicular to the beam. The main baffles could be welded, instead of riveted to the laminae of the collar.

In other words, they would efficiently redirect the desired fraction of the total helium flow through the annulus around the beam tube. In Fig. 5, these devices – yet to be designed in detail – have been schematically indicated by a varying diameter of yoke channels. (This should not be interpreted as a recommendation to design channel bores in the iron with varying diameters; they would probably be deleterious for the unformity of the magnetic field.)

The above arguments about achievable pressure differences could be criticized

on the grounds that Bernoulli's equation applies only to laminar flow. However, while one must distrust its quantitative use in the present context, qualitatively the arguments should be valid. After all, a simple water-jet vacuum pump works well in spite of the flow at the exit of its nozzle being turbulent.

The advantages of the proposed scheme of transverse cooling are

1. Minimal obstructions in the yoke channels, i.e., global insensitivity to potential interruption of helium flow around the beam tube in a single magnet.
2. The exploitation of the hydrodynamic pressure to ensure adequate helium flow in the annulus; this should permit the introduction of transverse cooling with a minimal increase of the external pressure differential.
2 Modularity, which practically guarantees longitudinally uniform cooling, except for the unavoidable saw-tooth variation with a 6-inch period of the temperature difference between helium in the annulus and helium in the yoke channels.

On paper, this would guarantee a temperature rise of the coil as low as 6 mK. This value would be increased somewhat by "leaks" [16], [17], i.e., imperfect return of warm helium to the yoke channels. However, the proposed scheme should work at least as well as the Shutt-Rehak method, i.e., guarantee a temperature rise of the coil of the order of 20 mK. Detailed calculations and tests would be needed to make a more reliable prediction.

The major disadvantage of the transverse cooling concept proposed here is the proliferation of baffles and obstructions inside the cold mass. A hybrid scheme, combining at least some of the advantages of the present concept and of the Shutt-Rehak method, might be feasible [11].

5. Metallic heat shunt

A metallic heat shunt serves to decrease as much as possible the thermal resistance between the beam tube and the helium in the yoke channels, without relying on helium flow around the beam tube. A prime consideration in its

design is practicality: its incorporation should necessitate only minor changes in the design of the cold mass. In particular, the nearly unavoidable mechanical weakening of the collar should be minimal. We adopt the criterion that this weakening may not exceed 10 %.

Many different metallic heat shunts are imaginable. Here, I present a simple one which may serve as a point of departure for better ideas. It requires two modifications of the present design:

1. The thermal resistance of the collar is decreased by coating the stainless steel laminae with copper*.
2. Heat is conducted from the beam tube to the inner collar surface by a copper sheet, longitudinally segmented to minimize eddy currents. This part of the heat shunt will be called the *inner* shunt.

The stainless steel collar has a large thermal resistance. A cylinder of length l, inner radius r_i, and outer radius r_o has a radial thermal resistance

$$R_{th} = \frac{\ln(r_o/r_i)}{2\pi k\, l} \ . \tag{5.1}$$

Cylinders made of stainless steel with inner/outer radii of 2cm/3cm, 3cm/4cm, and 4cm/5.5cm have radial thermal resistances R_{th} of, respectively, 35.2 'mK', 25.0 'mK', and 27.7 'mK'. The radial thermal resistances of cylindrical sections occupying an angular width $\Delta\Phi$ are larger than the above values by a factor $2\pi/\Delta\Phi$.

The collar is made of 1/16-inch-thick stainless steel laminae. It should be possible to coat them on both sides with 1 mil of copper. This would reduce the mechanical strength of the collar by about 3 % but decrease its thermal resistance by a factor of about 30. As seen in Fig. 7, the inner shunt should deliver heat to the collar effectively at the radius $r = 3$ cm. If heat has to

* This has been suggested by R. Schermer.

traverse the collar between $r = 3\,\mathrm{cm}$ and its external radius of $r = 5.5\,\mathrm{cm}$, about half of the total azimuthal angle of 2π is obstructed by the outer coil. The radial thermal resistance of the unobstructed part of the collar is thus $R_{th} \approx 2\,(25 + 28)/30$ 'mK'≈ 4 'mK'.

Unfortunately, it may well prove uneconomical to coat individual laminae, and they would have to be punched from coated sheets.* As a consequence, the heat current may be forced to pass through a few tenths of a millimeter of stainless steel before being able to enter copper. This could add a few 'mK' to the radial thermal resistance of the collar. Also, the heat flux in the iron yoke would be slightly more concentrated than in Fig. 3, increasing somewhat the temperature differential across the yoke. On the other hand, in recent design modifications of the collar [19], the gap between the collar and the yoke has been greatly reduced so that the corresponding temperature differential should be considerably smaller than quoted in Table 2. Thus, a fair estimate of the temperature differential between the outer surface of the innner shunt and the helium in the yoke channnels may be somewhere in the range 25-30 mK.

A cross section of the inner shunt is shown very schematically in Fig. 7. The shunt consists of a copper tube with four extending wings. The wings and the short parts of the tube connecting two adjacent wings at the polar plane (between the lines marked A) are the elements that transmit heat to the collar. The copper tube collects heat from the beam tube. The most important parameter of the inner shunt is its thickness t, which must be determined as a compromise between the conflicting requirements of minimal thermal resistance and minimal space occupancy. A compromise giving, if anything, more weight to the latter requirement is $t = 0.2\,\mathrm{mm}$. Using the simple calculational tools of Appendices A-C and a rough guess of potential azymuthal asymmetry of the heat flux entering the inner shunt from the beam tube, one arrives at 25 mK as a best estimate for the maximum temperature differential in the inner shunt. To first approximation,

* On the other hand, this would automatically suppress eddy currents.

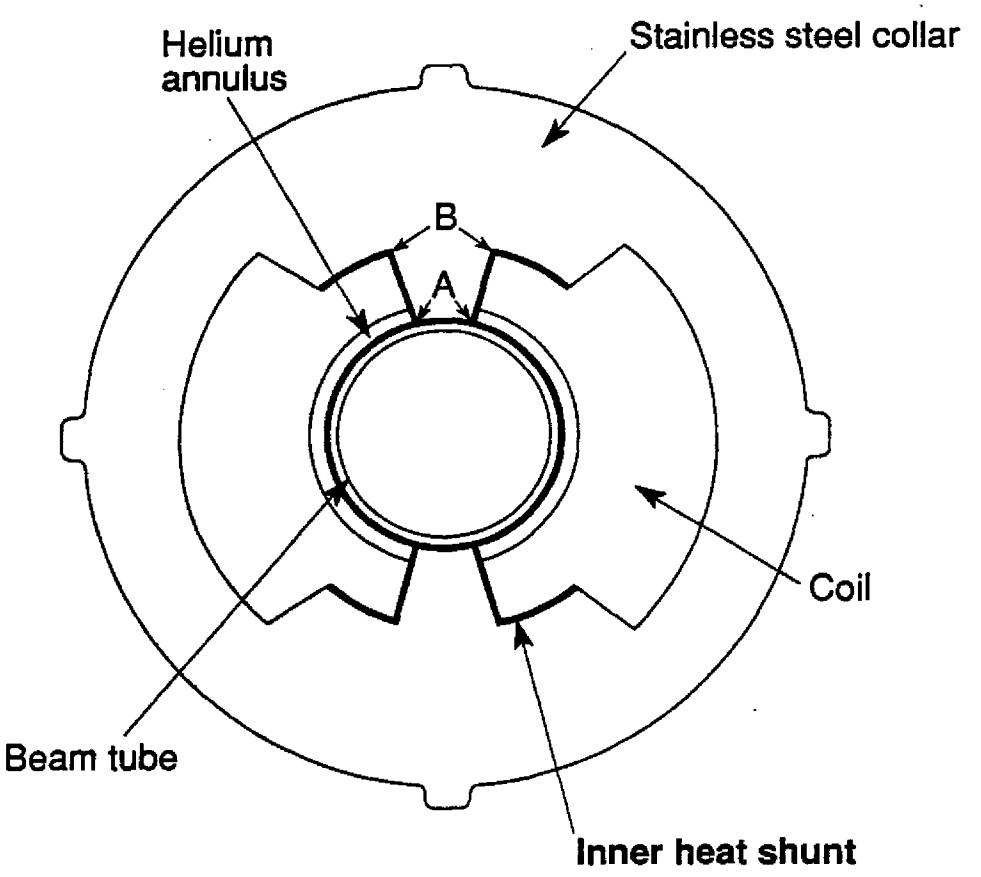

FIG. 7. A schematic cross section of the inner heat shunt. The thickness of the shunt is exagerated for good visibility. In the different designs discussed in the text, the shunt is either single- or double-layered between the lines (points in the drawing) marked A and B, respectively, and either double- or triple-layered between the two adjacent lines marked A. The lower half of the shunt is built in the same way as the upper half.

this temperature differential is linear in t. The necessary segmenting of the inner shunt may add a few mK, and a few mK more may be needed for the heat flux to traverse the boundary resistance between inner shunt and collar (see below). However, the warmest part of the superconductor is also a few mK cooler than the inner shunt at its warmest spot. Therefore, a fair estimate of the temperature rise of the coil is

$$\Delta T = 55 \text{ mK} ,$$

with a relative standard deviation of about 10%, to be compared with 155 mK in the present design (see Section 3).

Because of eddy currents, an inner shunt as thick as 0.2 mm would hardly be acceptable unless segmented. As explained in the CDR[1], the critical effect of eddy currents in the 0.05-mm-thick copper lining of the beam tube is mechanical stress during a quench. The proposed inner shunt does not have the backing of a 1-mm-thick stainless steel tube, and one may even require it to be self-supporting. Therefore, eddy currents should be reduced by the ratio of the yield strengths of stainless steel and copper, multiplied by the ratio $1\,\mathrm{mm}/0.05\,\mathrm{mm} = 20$. The ratio of yield strengths depends on the detailed composition and state of the two metals; we take it to be 30. Thus, eddy currents must be reduced by a factor of about 600. As shown in Appendix D, this can be achieved by slicing the inner shunt into 2-mm-long segments, except near the polar plane. There, the segments may be connected along two strips, one at the top and one at the bottom of the tube. Estimates show that the strips may also be about 2 mm wide. Note that these conclusions are independent of the thickness t of the inner shunt, for any reasonable value of t.

Clearly, the inner shunt as drawn in Fig. 7 is not a very practical device. On the way to its engineering design, some thermal and electrical requirements have to be kept in mind. From a thermal point of view, separating the inner shunt at midplane into an upper and a lower half does no harm. However, then it could not support itself under eddy currents. Separating the shunt at the polar plane into a left and a right half is a bad idea for thermal reasons, because it could no longer contribute to establish the left-right symmetry of the heat flux outside the cylindrical surface with $r = 2\,\mathrm{cm}$; as a consequence, the temperature rise of the coil could become substantially larger than the value of 55 mK estimated above.

We conclude that it is probably best to keep the copper tube (segmented on its sides) as a unity. It would be nice to have it supported on the outside by, e.g., another stainless steel tube; then one could tolerate considerably longer

segments. However, this alternative is probably acceptable only if an additional tube is required for other purposes (e.g., measurements of the magnetic field). Also, the thermal contact between the tube and the wings might be a more complicated problem than otherwise.

To have the copper tube supported by the inner coil is probably a bad idea. It might necessitate additional electrical insulation of the inner coil, thus also increasing its thermal insulation with respect to the helium in the annulus. While this may seem advantageous, in that it would better insulate the coil from the heat generated in the beam tube, it would be deleterious for the cooling of the coil after direct energy deposition in the superconductor, for instance by a hadronic shower.

A good alternative to a self-supporting copper tube may be a suitably segmented copper layer deposited on the outer surface of the beam tube (in case the latter is not equipped with correction coils). Another possibility is an additional thin tube made of any suitable material, either insulating or poorly conducting, with such a copper layer deposited on its *outer* surface. This would facilitate the establishment of a good thermal contact with the wings. Of course, any additional tube would take some more space, in a place where it is at a premium.

The simplest wings would consist of two *separate* segmented copper sheets, one at the top and one at the bottom, covering the inner surface of the collar at any radius $r \leq 3\,\mathrm{cm}$. Then one would have to rely on the wing-tube thermal contact along the narrow strip confined between the lines marked A in Fig. 7 and the corresponding strip at the bottom. This seems very risky: each mil of liquid helium in the gap between the wings and the copper tube would contribute nearly 10 mK to the temperature differential in the inner shunt.

Much more reliable ways to establish a good thermal contact between the wings and the tube are welding, brazing, or hard soldering [14]. However, the assembly of the cold mass would be considerably facilitated if the wings extended only to the lines marked B in Fig. 7. Indeed, this may suffice if, *in addition*, the

collar is equipped with the two sheets envisioned in the previous paragraph. The high mechanical pressure exerted by the collar on the inner coil along the surfaces between lines A and B should guarantee a very good thermal contact, while the sheets would efficiently transmit the heat flux to the collar.

The most extreme possibility is to have the wings in their full length attached (e.g., brazed) to the copper tube. Then they must be bent at the lines B after the coils are mounted on the beam tube. This might negatively affect their heat conductance.

In any of these schemes, a few tenths of a millimeter of stainless steel would have to be removed from the collar as presently designed, in order to accomodate the inner shield. Since this removal is required only in places where the collar is at least 2.5 cm thick, its ensuing additional weakening should be negligible.

The thermal performance of the shunt could easily be improved, for instance simply by making it thicker, but then one would have to start looking hard into all remaining thermal resistances between the beam tube and the helium in the yoke channels, and perhaps consider copper-coating the iron laminae of the yoke as well. However, a coil temperature rise of the order of 30 mK should be achievable, while still leaving sufficient space for a helium annulus, preferably between the inner shunt and the coil. Even lower values of the temperature rise are imaginable, if the thermal conductivity of the metal (copper or aluminum) turns out to be higher than assumed in this Note.

6. What to do next?

Probably, there is still plenty of room for good ideas on how to cool the beam tube. However, at some point, a decision must be made about which ideas are to be further pursued and what the final goal is. This decision will have to be followed by experimental research and development. It would be risky to start the mass production of magnets before their thermal behaviour has been tested on prototypes. This requires thermometry and a reliable method to deliver a known amount of heat to the beam tube. Some suggestions on the latter problem have

been made previously [20], [21]. In retrospect, I find them more or less sound* but too complicated.

A simpler method to test the cooling of the beam tube is based on the fact that heat conduction through a series of concentric cylindrical tubes in good thermal contact is well understood (see, for instance, Appendices A-C). Take as an example the cold mass as presently designed. Imagine an auxilliary insulating tube, copper-clad on its outside, snuggly fitting into the beam tube, and cooled by liquid helium flowing through its bore. By passing a current through the copper lining of the insulating tube,** a known amount of thermal power would be delivered. From the measured helium flows and the measured helium temperatures at entrance and exit, both in the cold mass and in the auxilliary tube, the thermal resistance of the cold mass could be calculated in units of the known thermal resistance of the auxilliary tube.

The problem with this method is the convective resistance between beam tube and auxilliary tube, which would have to be either separately measured or kept small. Also, we are interested more in the temperature rise of the coil than in the total thermal resistance of the cold mass. However, if the thermal resistance of the beam tube itself were known (for instance, in the case of a bare beam tube without insulating tapes, made of stainless steel with well-known thermal conductivity), this tube could be copper clad on its outside and used as described in the preceding paragraph. The external copper lining could consist of longitudinal strips, each carrying a different current so as to simulate an azimuthally nonuniform heat flux.

---

* Ref. [21] assumes the literal interpretation of Fig. 2, based on the questionable boundary condition discussed in Section 3. However, the present reinterpretation of Fig. 2 suffices to make the contents applicable except that, in principle, an iterative procedure might be necessary to find the heat flux to be injected into the stainless steel tube.

** The copper must be sufficiently thick so that the ohmic heating of the stainless steel is negligible.

7. Conclusions

It is both desirable and feasible to improve the cooling of the beam tube as compared to the present SSC design. Both transverse helium flow and a metallic heat shunt are promising approaches. They complement each other in their advantages and disadvantages. A metallic shunt is a passive device that cannot be disabled by clogging of the annulus or similar misfortunes. On the other hand, helium is a unique substance because of its large specific heat relative to other materials at low temperatures. A thorough analysis of the coil temperature variation after direct heat deposition in the superconductor would probably prove that some helium flow in the annulus is indispensable. Also, transverse helium flow may reduce the temperature rise of the coil to lower values than any reasonably dimensioned metallic shunt.

An attractive possibility is to combine transverse helium flow with a metallic heat shunt. It would offer the advantages of both cooling methods and, under some circumstances, lead to an even lower temperature rise than each method by itself. A value in the vicinity of or even below 20 mK does not seem out of the question.

None of these possibilities should detract attention from a search for insulating tapes with higher thermal conductivity than the presently used brand of Kapton. This search is as important as ever, because a tape with higher thermal conductivity would improve the cooling of the superconductor after direct energy deposition.

Naively, reducing the temperature rise of the coil with respect to the helium in the yoke channels to the level of 20 mK seems hardly worth the effort in view of the 170 mK temperature difference between the coldest and warmest helium in the yoke channels along an arc sector. However, the long time constants needed for a change of the helium temperature in the yoke channels make the latter difference less important than it seems. Again, to substantiate this remark, one would have to discuss the temporal response both of the superconductor

temperature after a sudden energy deposition, and of the chromaticity correctors in the accelerator.

Acknowledgements

The problem of beam-tube cooling has been suggested to me by T. Kirk and M. Tigner. I am indebted to them and to many other present and former members of the CDG, in particular to R. Carcagno, D. Jackson, P. Limon, M. McAshan, J. Peterson, R. Schermer, and R. Stiening for discussions and suggestions. D. Groom has graciously introduced me to the pleasures of the TEX typesetting system, but he is not responsible for my deficiency in its usage. Sincere thanks are due to K. Metropolis for painstakingly proofreading the manuscript and expurgating the worst examples of my broken English, except in some last-minute additions and alterations.

Appendix A. A one-dimensional approximation for a two-dimensional heat-conduction problem

Consider the time-independent heat-conduction problem presented in Fig. 8. The figure shows two slabs of infinite extent in the z-direction, length L in the x-direction, thicknesses t_1 and t_2 in the y-direction, and thermal conductivities k_1 and k_2, respectively. At the surface $y = 0$, the temperature T is fixed and normalized to $T = 0$. A heat flux with x-dependent density $j(x)$ [W/m^2] is injected into the upper slab at the surface $y = y_2$. The boundary conditions at the surfaces $x = 0$ and $x = L$ are yet to be specified.

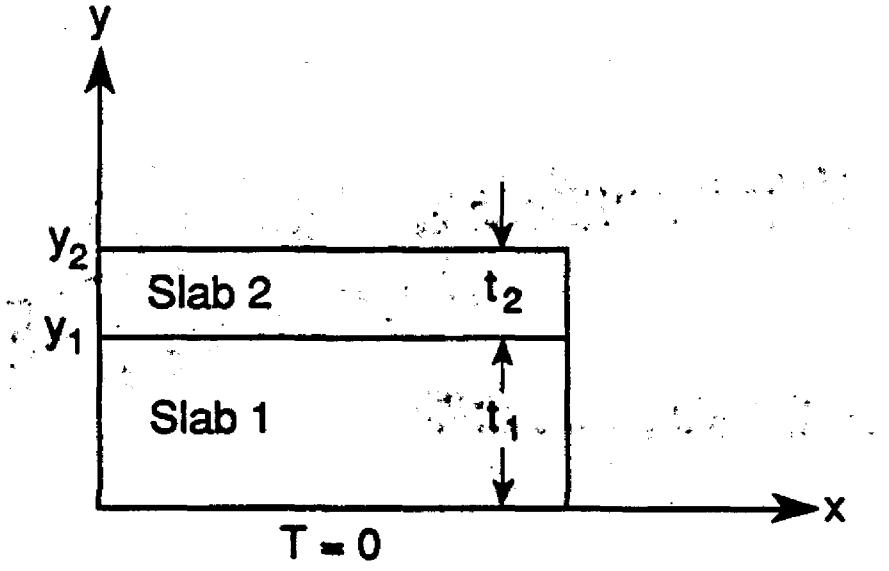

FIG. 8. The coordinate system and some of the notation used in the analysis of heat conduction in two slabs.

This is essentially the problem treated by Jackson [9] and Carcagno [5]. The differential equation for the temperature field is

$$\frac{\partial^2 T}{\partial x^2} + \frac{\partial^2 T}{\partial y^2} = 0 \,, \tag{A1}$$

and the boundary conditions are

$$T(y=0) = 0 \tag{A2a}$$

$$k_1 \frac{\partial T}{\partial y}\bigg|_{y=y_{1-}} = k_2 \frac{\partial T}{\partial y}\bigg|_{y=y_{1+}} \tag{A2b}$$

$$k_2 \frac{\partial T}{\partial y}\bigg|_{y=y_2} = j(x) \ . \tag{A2c}$$

Here, y_{1-} and y_{1+} designate the limits as y approaches y_1 from below and above, respectively.

Let us introduce the temperature $U(x)$ defined as the temperature in slab 2, averaged over its thickness

$$U(x) = \frac{1}{t_2} \int_{y_1}^{y_2} T(x,y)\, dy \ . \tag{A3}$$

By integrating eq (A1) with respect to y between y_1 and y_2 one obtains

$$\frac{d^2U}{dx^2} + \frac{1}{t_2}\left(\frac{\partial T}{\partial y}\bigg|_{y=y_2} - \frac{\partial T}{\partial y}\bigg|_{y=y_{1+}} \right) = 0 \ .$$

Using the boundary conditions (A2b) and (A2c) one gets

$$\frac{d^2U}{dx^2} + \frac{j(x)}{k_2 t_2} - \frac{k_1}{k_2 t_2} \frac{\partial T}{\partial y}\bigg|_{y=y_{1-}} = 0 \ . \tag{A4}$$

Until now, the calculations have been exact. At this point, we introduce the approximation

$$\frac{\partial T}{\partial y}\bigg|_{y=y_{1-}} \approx \frac{U(x)}{t_1} \ , \tag{A5}$$

which converts eq (A4) into

$$\frac{d^2U}{dx^2} + a(x) - \frac{U(x)}{b^2} = 0 \tag{A6}$$

with

$$a(x) = \frac{j(x)}{k_2 t_2} \tag{A7}$$

and

$$b = \sqrt{\frac{t_1 t_2 k_2}{k_1}} \, . \tag{A8}$$

The approximation is good if the temperature in slab 2 varies only slightly in the y-direction and if the heat current in slab 1 flows nearly in the y-direction. This is the case if the following sufficient conditions (perhaps not all of them necessary) are fulfilled:

a) $T(x, y = y_2) - T(x, y = y_1) \ll U(x)$ on the open x-interval $]0, L[$.

b) $k_1 \ll k_2$ (see Fig. 4 of the text).

c) $|dU/dx| \ll U(x)/t_1$ on the open x-interval $]0, L[$. The latter condition means that the temperature U changes appreciably only over distances that are large compared with thickness t_1 of slab 1. In general, its fulfillment will depend on the parameters of the problem, i.e., $a(x)$, b, and L. Often condition c) will be fulfilled if

c') $t_1 \ll b$ i.e. $k_1 t_1 \ll k_2 t_2$.

For instance, conditions *c*) and *c'*) are well fulfilled in the case of the copper-lined beam tube treated by Jackson and Carcagno using the full two-dimensional equation.

Appendix B. Solution of the one-dimensional problem

The general solution of eq (A6) for $a = 0$ (i.e., of the corresponding homogeneous equation) may be written in the form

$$U(x) = Ae^{x/b} + Be^{-x/b} \qquad \text{(for } a = 0\text{)} \ . \tag{B1}$$

A and B are integration constants; their value depends on the boundary conditions at the surfaces $x = 0$ and $x = L$.

An interesting case arises if $a(x)$ is a δ-function of x such that the solution (B1) of the homogeneous equation applies but the boundary conditions are

$$\begin{aligned} dU/dx\big|_{x=0} &= -J/(k_2 t_2) \\ dU/dx\big|_{x=L} &= 0 \ . \end{aligned} \tag{B2}$$

Here, J [W/m] is the (total heat flux)/(unit length in the z-direction) injected into slab 2. Then we have

$$U(x) = \frac{Jb}{k_2 t_2} \frac{\cosh[(L-x)/b]}{\sinh(L/b)} = U(0) \frac{\cosh[(L-x)/b]}{\cosh(L/b)} = U(L) \cosh[(L-x)/b]$$

$$U(0) = \frac{Jb}{k_2 t_2} \frac{1}{\tanh(L/b)} = J\sqrt{\frac{t_1}{k_1 k_2 t_2}} \frac{1}{\tanh(L/b)} \tag{B3}$$

$$U(L) = J\sqrt{\frac{t_1}{k_1 k_2 t_2}} \frac{1}{\sinh(L/b)} \ .$$

An interesting quantity is the temperature difference $DU(x) = U(0) - U(x)$ between the point $x = 0$ and any other point x in slab 2. We have, of course, $DU(0) = 0$ and

$$\begin{aligned} DU(x) &= U(0)\left(1 - \frac{\cosh[(L-x)/b]}{\cosh(L/b)}\right) \\ DU(L) &= U(0)\left(1 - \frac{1}{\cosh(L/b)}\right) \ . \end{aligned} \tag{B4}$$

The latter quantity is the maximum temperature drop in slab 2.

In two limiting cases, these expressions assume particularly simple and intuitively understandable forms:

a) $L/b \gg 1$

$$U(x) = U(0)e^{-x/b}\ , \qquad U(0) = J\sqrt{\frac{t_1}{k_1 k_2 t_2}}\ , \qquad U(L) = 0 \qquad (B3')$$

$$DU(x) = U(0)(1 - e^{-x/b})\ , \qquad DU(L) = U(0)\ . \qquad (B4')$$

Here, the temperature decreases exponentially with increasing x and approaches zero for large x; the "decay" constant is b. The maximum temperature $U(0)$ at $x = 0$ is the same as if the flux J were conducted through the good heat conductor 2 over a distance b. If one considers the properties of slab 1 as fixed and those of slab 2 as variable, $U(0) = DU(L)$ scales with $1/\sqrt{k_2 t_2}$.

b) $L/b \ll 1$

$$U(x) = U(0) = \frac{Jb^2}{k_2 t_2 L} = \frac{Jt_1}{k_1 L} \qquad \text{(to 1.order)} \qquad (B3'')$$

$$\begin{aligned} DU(x) &= \frac{U(0)\,x\,(L - x/2)}{b^2} = \frac{J\,x\,(L - x/2)}{k_2 t_2 L} \\ DU(L) &= \frac{U(0)L^2}{2b^2} = \frac{JL}{2k_2 t_2}\ . \end{aligned} \qquad \text{(to 2.order)} \qquad (B4'')$$

Here, the temperature along slab 2 is, to first order, constant; to second order it is a decreasing quadratic function of x with a minimum at $x = L$. The maximum temperature $U(0)$ is, to first approximation, the same as if the flux J were uniformly distributed over the entire slab length L; $U(0)$ scales to first order with $1/L$. However, $DU(L)/L$, i.e., the average temperature gradient in slab 2 scales with $1/(k_2 t_2)$.

From eq (B1), the general solution of eq (A6) may be obtained for any $a(x)$ by well-known methods. If $a(x) = a =$ const., i.e., $j(x) = j =$ const., the general

solution of eq (A6) is

$$U(x) = \frac{jt_1}{k_1} + Ae^{x/b} + Be^{-x/b} \ . \qquad (B5)$$

If, in addition, a flux J is withdrawn from slab 2 at $x = 0$, the boundary conditions (B2) apply but with the opposite sign of J. By comparison with eq (B3) one realizes that eq (B6) assumes the form

$$U(x) = \frac{jt_1}{k_1} - \frac{Jb}{k_2 t_2} \frac{\cosh[(L-x)/b]}{\sinh(L/b)} \ . \qquad (B6)$$

If $L/b \ll 1$, eq (B6) takes the limiting form

$$U(x) = \frac{(j - J/L)t_1}{k_1} + DU(x) \ , \qquad (B7)$$

with $DU(x)$ given by eq (B4$''$). This time, the temperature is maximal at $x = L$. There is a good physical reason for the quantity $DU(x)$ of eq (B4$''$) occurring in eq (B8). When heat is injected uniformly along slab 2 and conducted away at one of its ends, the temperature variation along the slab must be of opposite sign but otherwise of the same form as when heat is injected at one of its ends but conducted away uniformly over its length.

The function DU(x) of eq (B4$''$) in its second form is also a solution of the eigenvalue problem in $U'(x) \equiv dU/dx$, that arises from eq (A6) with its second term a constant and its third term put to zero, i.e.,

$$\frac{d^2U}{dx^2} + a = 0 \ , \qquad (B8)$$

combined with the boundary conditions (B2) but with the opposite sign of J. The eigenvalue is $a = J/(k_2 t_2 L)$.

This eigenvalue problem may be generalized for an arbitrary $a(x)$. Its solution is

$$U = U(0) + \left(x - \int_0^x c(u)\, du \right) F \ , \tag{B9}$$

with

$$c(x) = \frac{1}{F} \int_0^x a(u)\, du \tag{B10}$$

and

$$F = \left. \frac{dU}{dx} \right|_0 = \int_0^L a(u)\, du = \frac{J}{k_2 t_2} \ . \tag{B11}$$

As an example, if $a(x) = a(0)\ \cosh[(L-x)/h]$, one obtains

$$U(x) = U(0) + h^2\ a(0) \Big(\cosh(L/h) - \cosh[(L-x)/h] \Big) \tag{B9'}$$

$$c(x) = 1 - \frac{\sinh[(L-x)/h]}{\sinh(L/h)} \tag{B10'}$$

$$F = h\ a(0)\ \sinh(L/h) \ . \tag{B11'}$$

Since the eigenfunction determined by the eigenvalue problem is not directly U(x) but U′(x), the constant U(0) in eqs (B9) and (B9′) is still arbitrary. This reflects the separation of the original limiting solution for $L/b \ll 1$ into two terms of different order (cf. eqs (B3″) and (B4″)).

Appendix C. Generalizations

First, we remark that from the one-dimensional point of view the function $j(x)$ is the surface density of heat generated in slab 2. One may imagine generating it, for example, by electrical current, in which case one may have another slab 3 on top of slab 2 (see Fig. 8). If slab 3 has properties similar to slab 1, i.e., it fulfills conditions $a), b),$ and $c)$ of Appendix A, the treatment of Appendices A and B may easily be extended to the new situation with three slabs. Properties of slab 1 enter eq (A6) only via parameter b, where they appear in the combination $R(1) = t_1/k_1$, the thermal resistance per unit surface of slab 1. Slab 3 presents another thermal resistance in parallel with slab 1; therefore, $R(1)$ has to be replaced by

$$R(1,3 \text{ in parallel}) = \frac{1}{\mathrm{k_1/t_1 + k_3/t_3}} \ . \qquad (C1)$$

Similarly, if slab 3 with the required properties is placed below slab 1, and if the heat bath $T = 0$ is at the bottom of slab 3, the thermal resistances $R(1)$ and $R(3)$ act in series and $R(1)$ has to be replaced by

$$R(1,3 \text{ in series}) = \mathrm{t_1/k_1 + t_3/k_3} \ . \qquad (C2)$$

If the properties of either slab 1 or slab 2 vary in the x-direction, eq (A6) is not valid, in general. However, if these properties vary only little over a distance b, the solution of eq (A6) with an x-dependent b is still a good approximation to the exact solution of the two-dimensional heat-conduction problem. An even rougher approximation consists of solving eq (A6) with a constant b and introducing the x-dependence of b in the solution.

All such approximations essentially depend on the assumption that the heat current flowing from slab 1 into slab 2 at a given position x depends only on the temperature U at the same value of x, i.e., on assuming the essential correctness of eq (A5) albeit possibly with a different physical meaning of parameter t_1. This new t_1 divided by some new k_1 represents an "effective thermal resistance per unit

surface", which is a useful concept for qualitative reasoning. However, one has to be aware of the fact that, in general, a two-dimensional heat-conduction problem cannot be reduced to a one-dimensional problem. If one insists on talking about the quantity "thermal resistance per unit surface" under any circumstances, one has to accept the fact that its value may depend, e.g., on the choice of $j(x)$. When this dependence is strong for the range of different $j(x)$ of interest, the concept itself ceases to be useful.

It is of obvious interest to generalize the foregoing treatment to the analogous cylindrical problem presented in Fig. 9.

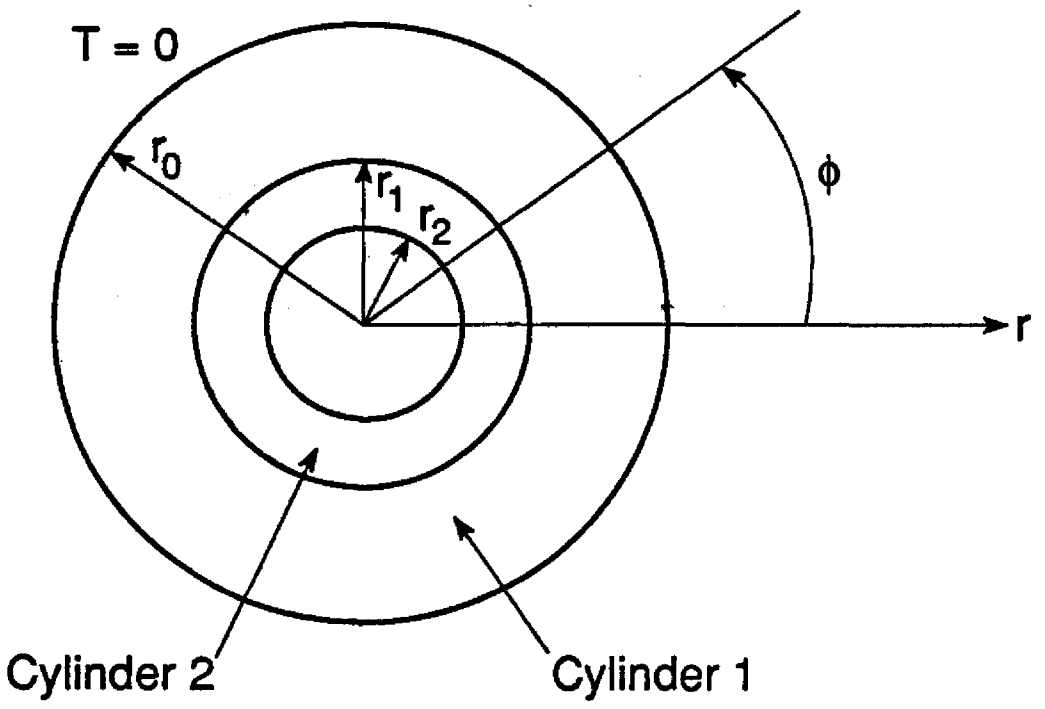

FIG. 9. The coordinate system and some of the notation used in the analysis of heat conduction in two concentric cylindrical shells.

The transformation

$$x = \phi \qquad y = -\ln \frac{r}{r_0} \tag{C3}$$

converts the two-dimensional Laplace equation in cylindrical coordinates r, ϕ into

eq (A1). The heat bath with temperature $T = 0$ is at $r = r_0$; i.e., eq (A2a) remains valid. The same is true of eq (A2b) but, obviously, in it we may replace y by r if desired. If we want to keep the physical meaning of the flux density $j(x)$, eq (A2c) has to be replaced by

$$k_2 \frac{\partial T}{\partial r}\bigg|_{r=r_2} = -j \tag{C4}$$

or

$$k_2 \frac{\partial T}{\partial y}\bigg|_{y=y_2} = j r_2 \ . \tag{C4'}$$

Eq (A3) now reads

$$U(x) = \frac{1}{y_2 - y_1} \int_{y_1}^{y_2} T(x,y)\, dy = \frac{1}{\ln r_1 - \ln r_2} \int_{r_2}^{r_1} T(x,y) dr/r \approx \frac{1}{t_2} \int_{r_2}^{r_1} T(x,y)\, dr \ . \tag{C5}$$

The approximation involved in writing the latter form is well justified if $t_2 \ll r_2$. Eq (A4) should be modified in that j is replaced by $r_2 j$ and t_2 is replaced by $y_2 - y_1$. Eq (A5) now reads

$$\frac{\partial T}{\partial y}\bigg|_{y=y_1-} \approx \frac{U(x)}{y_1 - y_0} \tag{C6}$$

so that eq (A6) remains in its original form but

$$a = \frac{r_2 j}{k_2(y_2 - y_1)} \approx \frac{r_2^2 j}{k_2 t_2} \tag{C7}$$

and

$$b = \sqrt{\frac{(y_1 - y_0)(y_2 - y_1)k_2}{k_1}} \approx \sqrt{\frac{(\ln r_0 - \ln r_1) t_2 k_2}{r_1 k_1}} \ . \tag{C8}$$

Again, the approximate forms of the above expressions are valid if $t_2 \ll r_2$. Notice that b is now dimensionless and a has the dimension of temperature, as

required in view of eq (C3). Since, with the above modifications, eq (A6) remains in its original form, so do its solutions. In particular, eq (B3) in the form

$$U(x) = \frac{Jr_2 b}{2k_2 t_2} \frac{\cosh[(\pi - x)/b]}{\sinh(\pi/b)} \tag{C9}$$

is the Green's function of the problem defined by eq (A6) and the boundary conditions

$$\begin{aligned} dU/dx\big|_{x=0} &= -Jr_2/(2k_2 t_2) \\ dU/dx\big|_{x=\pi} &= 0 \ . \end{aligned} \tag{C10}$$

Eq (C9) should be applied to azimuthal angles $\phi = x$ in the interval $[0, \pi]$, the values of U elsewhere being obtained from symmetry and periodicity requirements. The factor 2 in the denominator of eqs (C9) and (C10) is understandable since, contrary to the situation presented in Fig. 8, the total heat flux J divides itself in two: one half flowing towards positive x-values and another half flowing towards negative x-values. The temperature distribution $V(x)$ in slab 2 for the case of an arbitrary x-dependent $j(x)$ can be obtained from eq (C9) in the form

$$V(x) = \int_{x'=-\pi}^{x'=\pi} \frac{j(x')}{J} U(x - x')\, dx' \ . \tag{C11}$$

Appendix D. Eddy currents in a thin cylindrical shell of finite length

This calculation assumes a homogeneous external magnetic field $\vec{B}_{ext}$, with the constant time derivative $\dot{\vec{B}}_{ext}$ (constant in space and time!) perpendicular to the axis of a cylindrical shell of radius r and thickness $t \ll r$. It neglects all transient effects and could thus be called a "quasistatic" approximation. The extent of its validity will be investigated below. The geometry is presented in Fig. 10.

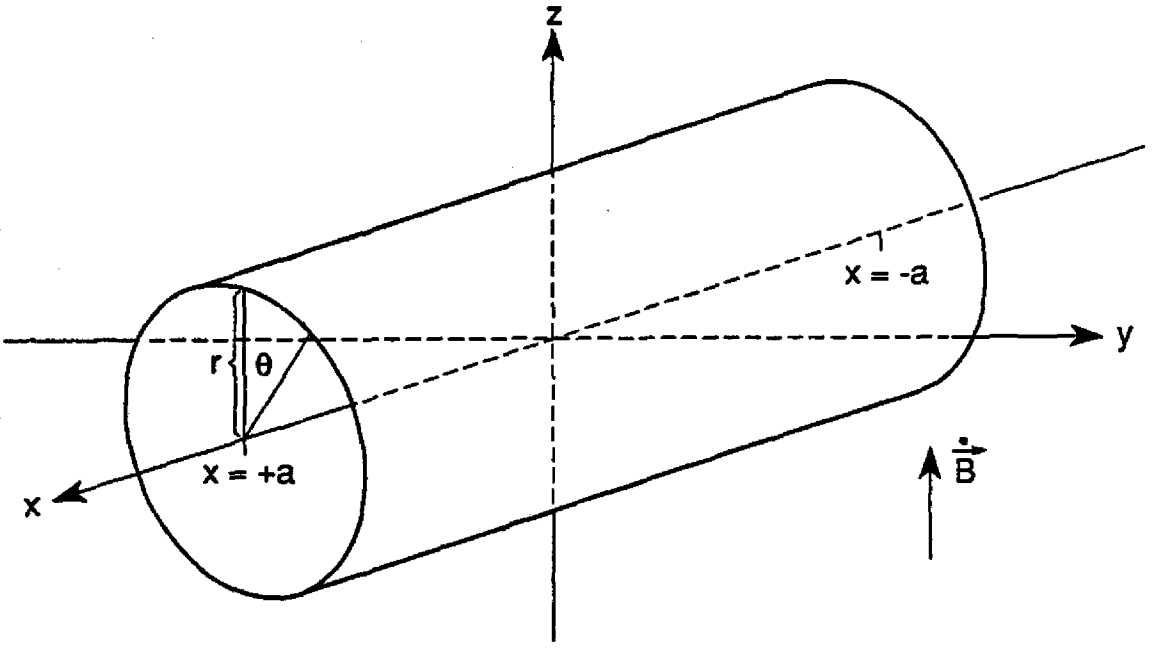

FIG. 10. The coordinate system and some of the notation used in the analysis of the cylindrical shell.

Maxwell's equations require

$$\operatorname{div} \vec{j} = 0 \tag{D1}$$

$$\operatorname{curl} \vec{E} = -\dot{\vec{B}}_{ext} \ , \tag{D2}$$

while Ohm's law states

$$\vec{j} = \sigma \vec{E} \ . \tag{D3}$$

In customary notation $\vec{j}$, $\vec{E}$, and σ designate the electrical current density, field, and conductivity. Combining eqs (D2) and (D3) yields

$$\mathrm{curl}\, \vec{j} = -\sigma \dot{\vec{B}}_{ext} \ . \tag{D4}$$

In cylindrical coordinates x, $\eta = r\theta$ $(-\pi \leq \theta \leq \pi)$, eq (D1) and the relevant component of eq (D4) read

$$\frac{\partial j_x}{\partial x} + \frac{\partial j_\eta}{\partial \eta} = 0 \tag{D5}$$

$$\frac{\partial j_x}{\partial \eta} - \frac{\partial j_\eta}{\partial x} = \sigma \dot{B}_{ext} \cos\theta \ . \tag{D6}$$

Here, j_η is defined as

$$j_\eta = j_y \cos\theta - j_x \sin\theta \ . \tag{D7}$$

In a cylinder of finite length $2a$ with its ends at $x = \pm a$, j_x has to be even in x and odd in η, while j_η has to be odd in x and even in η. Furthermore, $\vec{j}$ has to fulfill the boundary conditions

$$\begin{aligned} j_x(x = \pm a,\ \eta) &= 0 \qquad && \text{for any } \eta \\ j_\eta(x,\ \eta = \pm \frac{\pi}{2} r) &= 0 \qquad && \text{for any } x \ . \end{aligned} \tag{D8}$$

We define a new vector $\vec{i}$ by

$$\begin{aligned} i_x &= j_x - \sigma \dot{B}_{ext}\, r \sin\theta \\ i_\eta &= j_\eta \ . \end{aligned} \tag{D9}$$

It has the same symmetry properties as $\vec{j}$ but, instead of eq (D8), it fulfills the

boundary conditions

$$\begin{aligned} i_x(x=\pm a,\ \eta) &= -\sigma \dot{B}_{ext}\, r \sin\theta && \text{for any } \eta \\ i_\eta(x,\ \eta=\pm\frac{\pi}{2}r) &= 0 && \text{for any } x\ . \end{aligned} \tag{D10}$$

The vector $\vec{\imath}$ satisfies the two-dimensional equation

$$\left(\frac{\partial^2}{\partial x^2}+\frac{\partial^2}{\partial \eta^2}\right)\vec{\imath}=0\ , \tag{D11}$$

which has a solution

$$\begin{aligned} i_x &= -\frac{\sigma \dot{B}_{ext}\, r}{\cosh\frac{a}{r}}\cosh\frac{x}{r}\sin\theta \\ i_\eta &= -\frac{\sigma \dot{B}_{ext}\, r}{\cosh\frac{a}{r}}\sinh\frac{x}{r}\cos\theta \end{aligned} \tag{D12}$$

that fulfills both the required symmetry properties and the boundary conditions (D10); (do not forget that $\theta=\eta/r$!). From eq (D9) we obtain

$$\begin{aligned} j_x &= \frac{\sigma \dot{B}_{ext}\, r}{\cosh\frac{a}{r}}\left(\cosh\frac{a}{r}-\cosh\frac{x}{r}\right)\sin\theta \\ j_\eta &= -\frac{\sigma \dot{B}_{ext}\, r}{\cosh\frac{a}{r}}\sinh\frac{x}{r}\cos\theta\ . \end{aligned} \tag{D13}$$

The solution (D13) satisfies – miraculously enough – also eqs (D5) and (D6).

The total current I circulating in the upper (or lower) half of the shell is

$$I = t\int_0^r |j_x(x=0,\eta)|\, d\eta = t\int_0^a |j_\eta(x,\eta=0)|\, dx\ . \tag{D14}$$

Eq (D13) yields

$$I=\sigma \dot{B}_{ext}\, r^2 t\left(1-\frac{1}{\cosh\frac{a}{r}}\right)\ . \tag{D15}$$

Our main interest is to compare the maximum values of $|j_x|$ at constant r, $x=0$, and $|\theta|=\pi/2$ for two cases:

1. a long cylinder with $a = a_l \gg r$, and

2. a short cylinder with $a = a_s \ll r$.

We call these two values $j_x^{max}(\text{long})$ and $j_x^{max}(\text{short})$. We have

$$\begin{aligned} j_x^{max}(\text{long}) &= \sigma \dot{B}_{ext}\, r \\ j_x^{max}(\text{short}) &= \frac{\sigma \dot{B}_{ext}\, a_s^2}{2\, r} \ . \end{aligned} \tag{D16}$$

They are in the ratio

$$R_{max} \equiv \frac{j_x^{max}(\text{short})}{j_x^{max}(\text{long})} = \frac{a_s^2}{2\, r^2} \ . \tag{D17}$$

For the two cases, the ratio of total currents $R_{tot} \equiv I(\text{short})/I(\text{long}) = R_{max}$ is the same as given by eq (D17). Perhaps an even more relevant quantity to be compared with $j_x^{max}(\text{long})$ is the average j_x at $|\theta| = \pi/2$. One finds

$$R_{av} \equiv \frac{\frac{1}{2a}\int_{-a}^{+a} j_x(0, |\theta| = \pi/2; a = a_s \ll r)\, dx}{j_x^{max}(\text{long})} = \frac{a_s^2}{3\, r^2} \ . \tag{D18}$$

Eddy currents lead to volume force densities f, which cause stresses in the shell. The critical force density is the maximal radial force density f_r^{max} caused at $|\theta| = \pi/2$ by j_x in the external magnetic field $\vec{B}_{ext}$. Compared with that on a long shell, f_r^{max} on a short shell is reduced by the ratio R_{max} of eq (D17), and the average radial force density f_r^{av} at $|\theta| = \pi/2$ is reduced by the ratio R_{av} of eq (D18).

Eddy currents produce their own magnetic field $\vec{B}_{eddy}$, which, in principle, can be computed from eq (D13). However, we are not sufficiently motivated to carry through the rather tedious calculations. The main points can be made by evaluating only the maximal value of B_{eddy} at the center of the shell, i.e., at the origin of the coordinate system. There, $\vec{B}_{eddy}$ is antiparallel to $\dot{\vec{B}}_{ext}$ and has the

strength

$$B_{eddy}^{max} = \frac{\mu_0 \sigma \dot{B}_{ext}\, t\, r^2}{2 \cosh \frac{a}{r}} \left(r \int_0^a \frac{\cosh \frac{a}{r} - \cosh \frac{x}{r}}{R^3}\, dx + \int_0^a \frac{x \sinh \frac{x}{r}}{R^3}\, dx \right) \qquad (D19)$$

with $R^2 = x^2 + r^2$. The first and second integral represent the contributions of j_x and j_η, respectively. An analysis of the limiting value of B_{eddy}^{max} as $a \to \infty$ leads to the well-known expression

$$B_{eddy}^{max}(\text{long}) = \frac{\mu_0 \sigma \dot{B}_{ext}\, t\, r}{2} \ . \qquad (D20)$$

This originates uniquely from the $\cosh \frac{a}{r}$ term in the first integral of eq (D19). In the other extreme, for $a = a_s \ll r$, an expansion in x/r shows that

$$B_{eddy}^{max}(\text{short}) = \frac{\mu_0 \sigma \dot{B}_{ext}\, t\, a_s^3}{3\, r^2} \ . \qquad (D21)$$

In this case, j_x and j_η each contribute half of the above value, and the ratio with respect to $B_{eddy}^{max}(\text{long})$ is

$$R_{B,1} \equiv \frac{B_{eddy}^{max}(\text{short})}{B_{eddy}^{max}(\text{long})} = \frac{2\, a_s^3}{3\, r^3} \ . \qquad (D22)$$

Actually, of more interest than eq (D22) would be the analogous ratio comparing a single long shell with a long sequence of short adjacent shells, obtained by slicing the long shell into short segments. Without performing the calculation, one might guess that the j_η contributions of individual segments add to zero. The superposition of the j_x contributions of the segments certainly contributes a factor of the order r/a_s, and one may conjecture that

$$R_{B,many} \stackrel{?}{=} R_{av} = \frac{a_s^2}{3\, r^2} \ . \qquad (D23)$$

However, a slightly different numerical factor in the above equation would not be too surprising.

We are now in the position to estimate the validity of the quasistatic approximation. Clearly $\dot{\vec{B}}_{ext}$ cannot remain stationary forever. However, one may expect the quasistatic approximation to be a good one in cases when $\dot{\vec{B}}_{ext}$ varies sufficiently slowly. The question is how slow is "sufficiently" slow. If all important angular frequencies ω in the Fourier transform of $\dot{B}_{ext}$ are such that the amplitudes of the corresponding Fourier components are much larger than the analogous components of $\dot{B}^{max}_{eddy}$, the quasistatic approximation is expected to be valid.* For a long shell, eq (D20) leads to the condition

$$\omega \ll \frac{2}{\mu_0 \sigma t r} . \qquad (D24)$$

Since the skin depth at frequency ω may be defined as

$$t_{skin} = \sqrt{\frac{2}{\mu_0 \sigma \omega}} , \qquad (D25)$$

eq (D24) may also be expressed in the form

$$t r \ll t^2_{skin} \qquad \text{for a long shell .} \qquad (D26)$$

The analogous equations for a short shell and a segmented long shell are then

$$\frac{t a_s^3}{r^2} \ll t^2_{skin} \qquad \text{for a short shell} \qquad (D27)$$

and

$$\frac{t a_s^2}{r} \ll t^2_{skin} \qquad \text{for a long, segmented shell .} \qquad (D28)$$

The numerical factors have been omitted from the last two equations. We see that segmenting extends the low-frequency domain in which the quasistatic approximation is expected to be valid to higher frequencies. For instance, a long

* As usual in approximate calculations, one has to watch out for exceptions, such as quantities predicted to be zero in the approximation.

shell with $r = 2$ cm, $t = 0.2$ mm has a limiting parameter t_{skin}, as given by eq (D26), of 2 mm. If this shell is made of copper with a typical value of magnetic diffusivity $D_m = 1/(\mu_0\sigma) = 3 \times 10^{-4}\,\mathrm{m^2s^{-1}}$ at a temperature of 4.3° K and $B_{ext} = 6$ T, the corresponding limiting frequency ν, as given by eq (D25), is 24 Hz. The same shell segmented into 2 mm long sections has about 100 times higher limiting frequency. Thus, the quasistatic approximation may be of interest even in some conventional electrotechnical problems of eddy-current prevention.

We close with two more pedagogical remarks. First, in most magnetostatic problems, Ohm's law leads to electrostatic fields $\vec{E}_{stat}$ that obey curl $\vec{E}_{stat} = 0$ and, therefore, never produce an electromotive force. For instance, such electrostatic fields must arise between the adjacent segments of a sliced cylindrical shell, i.e., charges are induced at the ends of a segment. If one forgets this fact, one easily arrives at the obviously false conclusion that curl $\vec{E}$ between the segments is much larger and directed in the opposite direction from everywhere else. Similar problems occur in simpler, completely static situations; for instance, which are the electric charges on the surface of a direct-current-carrying wire of arbitrary shape far away from the source of electromotive force? *

Second, the assertion that eddy currents in a thin cylindrical shell are "miraculously" simple (at least in the quasistatic approximation) should be substantiated. The analogous problem in a rectangular parallelepiped can be solved by a method similar, but not identical, to the one presented here. The origin of the coordinate system is placed at the center of the parallelepiped, and its sides of lengths $2a$, $2b$, and $2c$ are aligned parallel to the x, y, and z axis, respectively. The constant time derivative $\dot{\vec{B}}_{ext}$ of the external magnetic field is directed along

* I have not yet found a standard textbook on electromagnetism treating such problems; although, admittedly, they are of little practical importance, they often cause considerable conceptual difficulties.

the z-axis.* The current density $\vec{j}$ is given by $j_z = 0$ and

$$
\begin{aligned}
j_x &= \sum_{n=0}^{\infty} j_n^x \cos(k_n x) \sinh(k_n y) \\
j_y &= \sum_{n=0}^{\infty} j_n^y \cos(l_n y) \sinh(l_n x)
\end{aligned}
\tag{D29}
$$

with

$$
\begin{aligned}
k_n &= (2n+1)\,\frac{\pi}{2\,a} \\
l_n &= (2n+1)\,\frac{\pi}{2\,b}
\end{aligned}
\tag{D30}
$$

and

$$
\begin{aligned}
j_n^x &= \quad 2\sigma \dot{B}_{ext}\, a\, \frac{(-1)^n}{(a k_n)^2 \cosh(k_n b)} \\
j_n^y &= -2\sigma \dot{B}_{ext}\, b\, \frac{(-1)^n}{(b l_n)^2 \cosh(l_n a)} \; .
\end{aligned}
\tag{D31}
$$

It can be easily checked that this solution has the correct limiting properties, e.g., that the current lines at small x, y are ellipses, or circles in case $a = b$. In the latter case $|\vec{j}|$ has the known value $|\vec{j}| = \sigma \dot{B}_{ext}\, r/2$.

A comparison of these results with the previous ones for a thin cylindrical shell lets us appreciate the simplicity of the latter. A more detailed analysis reveals some interesting qualitative differences between the shell and the parallelepiped in their response to segmenting.

* Due to the linearity of the problem, the solution for any other direction of $\dot{\vec{B}}_{ext}$ can easily be obtained by superposition.

References

1. SSC Central Design Group, "Conceptual Design of the Superconducting Super Collider", SSC-SR-2020, March 1986.

2. J.D.Jackson, "Short Sample Dipole Field versus Temperature for Different Copper to Superconductor Ratios", SSC-N-371, 8/4/1987.

3. J.Rasson, "Steady State Simulation of the SSC Magnet Cooling Circuit", SSC-N-523, June 1988.

4. General Dynamics, "Integrated Thermal Model of the Production Dipole Magnets for the Superconducting Supercollider", GDC PIN No.87-P-S001, October 1987; General Dynamics, "Thermal Parametric Studies of the Production Dipole Magnets for the Superconducting Supercollider", GDC PIN No.87-P-085D, April 1988; G.E.Hardy,S.D.Peck,"Integrated Thermal Analysis of the Production Dipole Magnets for the Superconducting Super Collider", SSC-N-554, September 1988.

5. R.Carcagno, "Temperature Rise in the SSC Dipole Coils under Synchrotron Radiation Heating", SSC-N-514, 5/27/1988.

6. A.W.Chao and J.M.Peterson, "Tolerance of Recooler Temperature from Persistent Current Effects", SSC-N-62-A, March 1986.

7. H.T.Edwards, "The Tevatron Energy Doubler: A Superconducting Accelerator", *Ann. Rev. Nucl. Part. Sci.* **35** (1985) 605.

8. M.K.Wilson, *Superconducting Magnets*, Oxford University Press, 1983.

9. J.D.Jackson, "Conduction of Heat of Synchrotron Radiation through the Wrapped Beam Tube Wall", SSC-N-235, September 1986.

10. M.McAshan, Memo to V.Karpenko and N.Goldwasser, 10/8/1987.

11. R.Carcagno, private communication.

12. W.M.Kays, *Convective Heat and Mass Transfer*, McGraw-Hill, 1966.

13. O.V.Lounasmaa, *Experimental Principles and Methods below 1 K*, Academic Press, 1974.

14. R.C.Richardson and E.N.Smith, *Experimental techniques in condensed matter physics at low temperatures*, Addison-Wesley, 1988.

15. R.P.Shutt, "SSC Magnet Cooling Reconsidered", SSC-N-522, 5/27/1988.

16. R.P.Shutt, "SSC Magnet Cooling by Transverse Liquid Helium Flow", Contribution to the Dipole Coil Insulation and Cooling Discussion Group, Brookhaven National Laboratory, February 15-16, 1989.

17. M.Rehak, "Heat Flow Calculations", Contribution to the Dipole Coil Insulation and Cooling Discussion Group, Brookhaven National Laboratory, February 15-16, 1989.

18. Č.Zupančič, "Cooling of the Bore Tube by Transverse Helium Flow", Internal Magnet Division Note, 2/12/1989, and Contribution to the Dipole Coil Insulation and Cooling Discussion Group, Brookhaven National Laboratory, February 15-16, 1989.

19. R.Schermer, private communication

20. Č.Zupančič, "How to Simulate (in Hardware) the Irradiation of the SSC Beam Tube by Synchrotron Radiation?", Internal Magnet Division Note, 11/2/1988

21. Č.Zupančič, "A 'Fast' Hardware Simulation of Synchrotron Radiation (SR)", Internal Magnet Division Note, 11/16/1988